arXiv:2212.14454v1 [cs.AI] 29 Dec 2022

MEAformer: Multi-modal Entity Alignment Transformer for Meta Modality Hybrid

Zhuo Chen, **Jiaoyan Chen**, **Wen Zhang**, **Lingbing Guo**, **Yin Fang**, **Yufeng Huang**, **Yuxia Geng**, **Jeff Z. Pan**, **Wenting Song** and **Huajun Chen**†

Abstract

As an important variant of entity alignment (EA), multi-modal entity alignment (MMEA) aims to discover identical entities across different knowledge graphs (KGs) with multiple modalities like images. However, current MMEA algorithms all adopt KG-level modality fusion strategies but ignore modality differences among individual entities, hurting the robustness to potential noise involved in modalities (e.g., unidentifiable images and relations). In this paper we present MEAformer, a **m**ulti-modal **e**ntity **a**lignment trans**former** approach for meta modality hybrid, to dynamically predict the mutual correlation coefficients among modalities for instance-level feature fusion. A modal-aware hard entity replay strategy is also proposed for addressing vague entity details. Extensive experimental results show that our model not only achieves SOTA performance on multiple training scenarios including supervised, unsupervised, iterative, and low resource, but also has limited parameters, optimistic speed, and good interpretability. Our code will be available soon.

1 Introduction

Recent years the knowledge graphs (KGs) have supported many AI applications like question answering [Chen *et al.*, 2021] and recommender systems [Gao *et al.*, 2022a] for commonsense knowledge and reasoning capabilities. As a critical task in KG integration and construction, entity alignment (EA) aims to identify equivalent entities across KGs against challenges such as distinct naming rules and multilingualism. Considering that those visual contents on the Internet can be used as a supplementary information of EA, multi-modal EA (MMEA) is proposed where each entity is attached with relevant images [Chen *et al.*, 2020a]. Current MMEA methods mainly focus on designing a suitable cross-KG modality fusion paradigm. [Liu *et al.*, 2021] learn modality-specific attention weights for modality importance. [Chen *et al.*, 2022] integrate visual features to guide relational and attribute feature learning. While [Lin *et al.*, 2022] apply the KL divergence over the output distribution between joint embedding and uni-modal embedding to reduce the modality gap. However, those algorithms all learn KG-level weights for modality fusion, but disregard the feature discrepancies (e.g., node degrees or relation numbers) and modality preferences (e.g., modality absence or ambiguity) for each entity across the KGs. These flaws somehow affect their robustness.

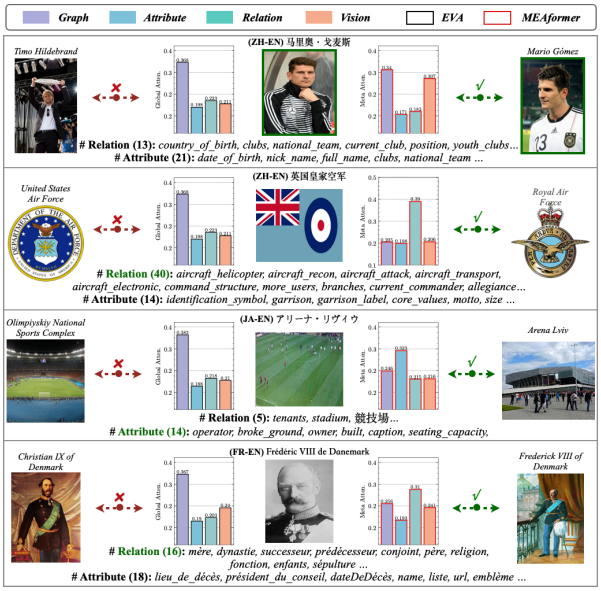

Figure 1: Some MMEA cases from DBP15K with weights of modalities by EVA [Liu *et al.*, 2021](left) and MEAformer (right).

Inspired by meta learning [Hospedales *et al.*, 2022], in this work, we explore an alternative paradigm to MMEA to encourage the emergence of adaptive meta modality weight, which focuses on generating reasonable instance-level multi-modal entity hybrid feature. Specifically, we propose a novel **m**ulti-modal **e**ntity **a**lignment trans**former** approach named MEAformer, which dynamically predicts mutual relatively weights among modalities for each entity pair (see examples in Figure 1). We implement our model as a meta learning alike paradigm, where our proposed dynamic cross-modal weighted (DCMW) module generates the meta weights for modality correction which enables inter-modal mutual rating though a shallow cross-attention network. Besides, we adopt a modal-adaptive contrastive learning objective to sufficiently disentangle the modality information with limited pre-aligned

entities, and a modal-aware hard entity replay is proposed to further strengthen model's robustness on vague entity details. Overall, the contributions can be summarized as:

- Our method can be seen as revisiting the MMEA works on the instance level, which has attracted only very limited attention so far.
- Our experiments show that MEAformer is able to achieve SOTA performance on multiple training scenarios with simple framework, limited parameters, optimistic speed, and good interpretability.

2 Related Work

Entity Alignment (EA) aims to discover equivalent entities among different KGs to facilitate knowledge fusion. Early EA systems exploit techniques such as logical reasoning and lexical matching for entity mapping construction [Jiménez-Ruiz and Grau, 2011; Suchanek *et al.*, 2011], highly relying on (ad-hoc) heuristics. Recent embedding-based EA methods alleviate the heterogeneity problem by learning an embedding space to represent those to-be-aligned KGs, where similar entities are kept close together while dissimilar ones are separated far apart. We divide them into two categories [Zhang *et al.*, 2022]: ***(i)*** *GNNs-based EA methods* [Sun *et al.*, 2020; Liu *et al.*, 2020; Wu *et al.*, 2020; Gao *et al.*, 2022b] mainly utilize graph neural networks (GNNs) like GCN [Kipf and Welling, 2017] and GAT [Velickovic *et al.*, 2018] for neighborhood entity feature aggregation. ***(ii)*** *Translation-based EA methods* [Zhang *et al.*, 2019; Sun *et al.*, 2019; Xin *et al.*, 2022; Cai *et al.*, 2022] use those translation-based KG embedding methods like TransE [Bordes *et al.*, 2013] to capture the entity structure information from relational triples.

Commonly, an alignment objective (e.g., embedding cosine similarity) is utilized on pre-aligned entity pairs (a.k.a. seed alignments) to calibrate KGs' semantic space in those methods. Also, the EA progress could be enhanced through additional strategies like: parameter sharing [Zhu *et al.*, 2017] (i.e., sharing the entity embedding of seed alignments across KGs); iterative learning [Sun *et al.*, 2018] (i.e., iteratively labeling entity pairs as pseudo seed supervision); attribute value encoding [Trisedya *et al.*, 2019]; collective stable matching for interdependent EA decisions [Zeng *et al.*, 2020]; explicitly linking the seed alignments among multiple heterogeneous KGs [Zhu *et al.*, 2017]; or guiding the entity matchings by ontological schemas [Xiang *et al.*, 2021].

Multi-modal Entity Alignment. Since being introduced by [Liu *et al.*, 2019] as a task of the multi-modal knowledge graph (MMKG) construction, incorporating the visual modality for EA in KGs gradually attracted the attention in communities with the development of multi-modal learning in recent years. [Chen *et al.*, 2020a] fuse the knowledge representations of modalities and then minimize the distance between the holistic embeddings of aligned entities. [Liu *et al.*, 2021] apply a learnable attention weighting scheme to give each modality various importance. [Chen *et al.*, 2022] integrate visual features to guide relational feature learning meanwhile assign weights to valuable attributes for alignment. While [Lin *et al.*, 2022] further enhance intra-modal learning via the contrastive learning and apply the KL divergence over the output distribution between joint embedding and uni-modal embedding to reduce the modality gap. However, all those methods ignore the dynamic of the inter-modal effects among all modalities, which is non-negligible in real world EA scenario since there are inevitable errors and noise in KGs (especially MMKGs) on the Internet or specific domains, e.g., containing unidentifiable images. Besides, the feature discrepancies (e.g., node degrees) and modality preferences (e.g., modality absence or imbalance) also frequently exist for entities. In this work, we propose an effective method MEAformer, which offers a fully dynamic meta modality hybrid strategy to solve the above problems.

3 Method

We define a MMKG as a five-tuple, i.e., $\mathcal{G}=\{\mathcal{E}, \mathcal{R}, \mathcal{A}, \mathcal{V}, \mathcal{T}\}$. $\mathcal{E}, \mathcal{R}, \mathcal{A}$ and $\mathcal{V}$ denote the sets of entities, relations, attributes, and images, respectively. $\mathcal{T} \subseteq \mathcal{E} \times \mathcal{R} \times \mathcal{E}$ is the set of relation triples. Given two MMKGs $\mathcal{G}_1 = \{\mathcal{E}_1, \mathcal{R}_1, \mathcal{A}_1, \mathcal{V}_1, \mathcal{T}_1\}$ and $\mathcal{G}_2 = \{\mathcal{E}_2, \mathcal{R}_2, \mathcal{A}_2, \mathcal{V}_2, \mathcal{T}_2\}$, MMEA aims to identify each pair of entities (e^1, e^2), $e^1 \in \mathcal{E}_1, e^2 \in \mathcal{E}_2$ where e^1 and e^2 represent the same real-world entity. Each entity is associated to multiple attributes and $0 \sim 1$ image. A set of pre-aligned entity pairs $\mathcal{S}$ (seed alignments) are offered for training guidance, and we assign $\mathcal{M}$ as the set for available modalities.

3.1 Multi-modal Knowledge Embedding

This section elaborates how we embed each modality of an entity into a low-dimensional vector in the given MMKGs.

Graph Neighborhood Structure Embedding. As a typical neural network, GAT is utilized to model the structural information of $\mathcal{G}$. Let $h_i \in \mathbb{R}^d$ be the hidden state of entity e_i, we denote the neighbor aggregating progress as :

$$h_i = RELU\left(\sum\nolimits_{j \in \mathcal{N}_i^{nb}} \alpha_{ij} \boldsymbol{W}_g h_j\right), \tag{1}$$

where $\mathcal{N}_i^{nb}$ is the first-order neighbors of e_i (including e_i), $\boldsymbol{W}_g \in \mathbb{R}^{d \times d}$ denotes a diagonal weight matrix [Yang *et al.*, 2015] for linear transformation, and α_{ij} is an attention weight between entity pair (e_i, e_j) which is expressed as:

$$\alpha_{ij} = \frac{\exp\left(LeakyReLU\left(\psi^\top\left[\boldsymbol{W}_g h_i \oplus \boldsymbol{W}_g h_j\right]\right)\right)}{\sum_{n \in \mathcal{N}_i^{nb}} \exp\left(LeakyReLU\left(\psi^\top\left[\boldsymbol{W}_g h_i \oplus \boldsymbol{W}_g h_n\right]\right)\right)}, \tag{2}$$

where $\psi \in \mathbb{R}^{2d}$ is the learnable weight and $\oplus$ refers to the concatenation operation. Multi-head strategy is applied to generate several (=2) independent representation h_i on each layer of GAT for learning stabilization. We simply average those h_i^k to constitute the embedding h_i^g of entity e_i in each layer, and denote the output h^g of the last GAT layer (=2) as the graph neighborhood structure embedding.

Relation, Attribute, Visual, and Surface Embedding. In order to avoid the information pollution brought by mixing relations and attributes representation in GNN network [Liu *et al.*, 2021], we apply the simple fully connect layers parameterized by $\boldsymbol{W}_m \in \mathbb{R}^{d_m \times d}$ to transform those features x^m:

$$h^m = FC_m(x^m), \ \ m \in \{r, a, v, s\}, \tag{3}$$

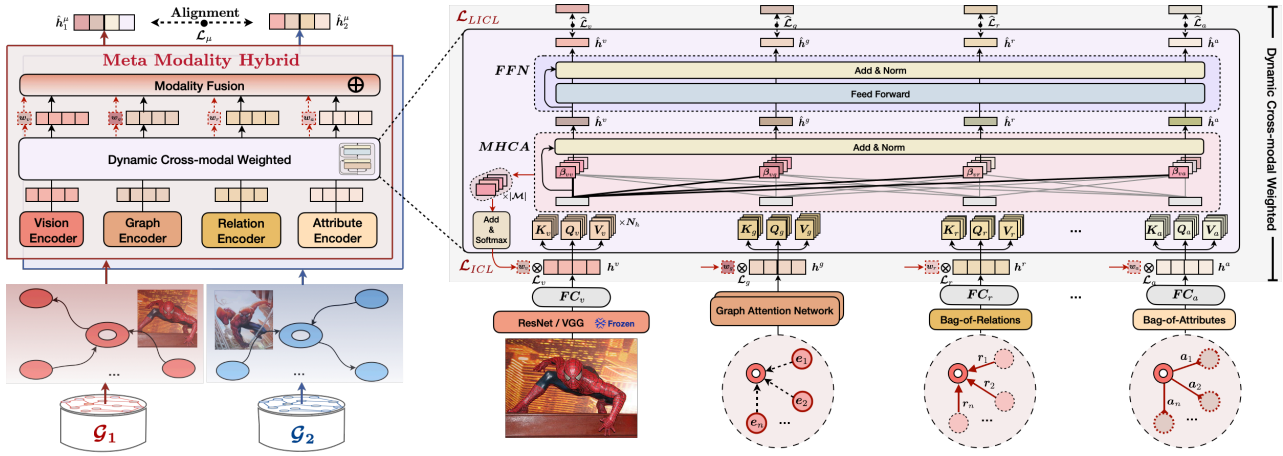

(a) MEAformer. (b) Implementation details for Meta Modality Hybrid.

Figure 2: (a) The overall framework of MEAformer and (b) the implementation details of meta modality hybrid (MMH).

where r, a, v, s represent the relation, attribute, vision, and surface (a.k.a. name string) modality, respectively. Besides, $x^m \in \mathbb{R}^{d_m}$ is the entity's input feature for modality m.

Note that we select the typical pre-trained visual model as the encoder (Enc_v) to get the visual embeddings for each image v_i of the entity e_i with the final layer output before logits as the image feature:

$$x_i^v = Enc_v(v_i)\,. \tag{4}$$

3.2 Meta Modality Hybrid

This section presents the meta modality hybrid (MMH) module, which enables the dynamic modality fusion for entities.

Dynamic Cross-modal Weighted (DCMW) aims to dynamically generate the instance-level meta weight for the feature from each modality. Inspired by the vanilla transformer [Vaswani *et al.*, 2017], we involve two types of sub-layers in DCMW: the multi-head cross-modal attention (MHCA) block and the fully connected feed-forward network (FFN).

Specifically, MHCA performs the attention function in parallel over N_h heads where the i-th head is parameterized by modally shared $\boldsymbol{W}_q^{(i)}$, $\boldsymbol{W}_k^{(i)}$, $\boldsymbol{W}_v^{(i)} \in \mathbb{R}^{d\times d_h}$ to project the multi-modal input h^m into modal-aware querie $Q_m^{(i)} \in \mathbb{R}^{d_h}$, key $K_m^{(i)} \in \mathbb{R}^{d_h}$, and value $V_m^{(i)} \in \mathbb{R}^{d_h}$:

$$Q_m^{(i)}, K_m^{(i)}, V_m^{(i)} = h^m\boldsymbol{W}_q^{(i)}, h^m\boldsymbol{W}_k^{(i)}, h^m\boldsymbol{W}_v^{(i)}\,. \tag{5}$$

For the feature of modality m, its output is:

$$\mathrm{MHCA}(h^m) = \left[\mathrm{head}_1^m \oplus \cdots \oplus \mathrm{head}_{N_h}^m\right]\boldsymbol{W}_o\,, \tag{6}$$

$$\mathrm{head}_i^m = \sum\nolimits_{j\in\mathcal{M}} \beta_{mj}^{(i)} V_j^{(i)}\,, \tag{7}$$

where $\boldsymbol{W}_o \in \mathbb{R}^{d\times d}$. The attention weight between entity's modality m and j in each head (β_{mj}) is formulated below:

$$\beta_{mj} = \frac{\exp(Q_m^\top K_j/\sqrt{d_h})}{\sum_{i\in\mathcal{M}}\exp(Q_m^\top K_i/\sqrt{d_h})}\,, \tag{8}$$

where $d_h = d/N_h$. Besides, layer normalization (LN) and residual connection (RC) are used to stabilize the training:

$$\hat{h}^m = LayerNorm(\mathrm{MHCA}(h^m) + h^m)\,. \tag{9}$$

FFN consists of two linear transformation layers with a ReLU activation function and LN&RC put behind as follows:

$$\mathrm{FFN}(\hat{h}^m) = ReLU(\hat{h}^m\boldsymbol{W}_1 + b_1)\boldsymbol{W}_2 + b_2\,, \tag{10}$$

$$\hat{h}^m = LayerNorm(\mathrm{FFN}(\hat{h}^m) + \hat{h}^m)\,, \tag{11}$$

where $\boldsymbol{W}_1 \in \mathbb{R}^{d\times d_{in}}$ and $\boldsymbol{W}_2 \in \mathbb{R}^{d_{in}\times d}$. We note that FFN is an optional component in our MEAformer since sometimes reducing parameters could alleviate the overfitting when the data is less complex (e.g., fewer attribute types).

Notably, we define the output meta modal weight w_m for each modality m as:

$$w_m = \frac{exp(\sum_{j\in\mathcal{M}}\sum_{i=0}^{N_h}\beta_{mj}^{(i)}/\sqrt{|\mathcal{M}|\times N_h})}{\sum_{k\in\mathcal{M}}exp(\sum_{j\in\mathcal{M}}\sum_{i=0}^{N_h}\beta_{kj}^{(i)}\sqrt{|\mathcal{M}|\times N_h})}\,, \tag{12}$$

which contains the crucial information about the inter-modal interface and adaptively adjusts our model's focus on different modalities for each entity.

Modality Fusion. Let w_m^i be the meta modal weight of entity e_i for modality m, we formulate the joint embedding as:

$$h_i^\mu = \bigoplus\nolimits_{m\in\mathcal{M}}[w_m^i h_i^m]\,,\quad h_i^\xi = \bigoplus\nolimits_{m\in\mathcal{M}}[w_m^i \hat{h}_i^m]\,, \tag{13}$$

where h_i^μ and h_i^ξ are defined as the early fusion and late fusion embedding, respectively. Note that the meta modal weight w_m^i is constantly changing across entities, and we select h_i^μ as the final entity representation for all evaluations.

3.3 Modal-adaptive Contrastive Learning.

In this section we introduce modal-adaptive contrastive learning (MACL) which aims to sufficiently mine the information contained in each modality with the given seed alignments $\mathcal{S}$.

Specifically, we corrupt the seed alignments (entity pairs) for negative alignments, following the 1-to-1 alignment assumption which is used in many EA works such as [Sun *et al.*, 2018]. For each seed alignment (e_i^1, e_i^2) in $\mathcal{S}$, we define $\mathcal{N}_i^{ng} = \{e_j^1 | \forall e_j^1 \in \mathcal{E}_1, j \neq i\} \cup \{e_j^2 | \forall e_j^2 \in \mathcal{E}_2, j \neq i\}$ as its negative set. Moreover, we involve the in-batch negative sampling strategy [Chen *et al.*, 2020b] which limits the sampling

	Models	Para.	DBP15K$_{ZH-EN}$			DBP15K$_{JA-EN}$			DBP15K$_{FR-EN}$		
			H@1	H@10	MRR	H@1	H@10	MRR	H@1	H@10	MRR
w/o SF	AlignEA [Sun *et al.*, 2018]	-	.472	.792	.581	.448	.789	.563	.481	.824	.599
	KECG [Li *et al.*, 2019]	-	.478	.835	.598	.490	.844	.610	.486	.851	.610
	MUGNN [Cao *et al.*, 2019]	-	.494	.844	.611	.501	.857	.621	.495	.870	.621
	AliNet [Sun *et al.*, 2020]	-	.539	.826	.628	.549	.831	.645	.552	.852	.657
	EVA* [Liu *et al.*, 2021]	13.3M	.680	.910	.762	.673	.908	.757	.683	.923	.767
	MSNEA* [Chen *et al.*, 2022]	14.1M	.601	.830	.684	.535	.775	.617	.543	.801	.630
	MCLEA* [Lin *et al.*, 2022]	13.2M	.715	.923	.788	.715	.909	.785	.711	.909	.782
	MEAformer (Ours)	13.7M	**.771**	**.951**	**.835**	**.764**	**.959**	**.834**	**.770**	**.961**	**.841**
	w/ MERP	13.7M	**.772**	**.951**	**.835**	**.769**	**.961**	**.840**	**.771**	**.962**	**.841**
w/ SF	RDGCN [Wu *et al.*, 2019]	-	.708	.846	–	.767	.895	–	.886	.957	–
	AttrGNN† [Liu *et al.*, 2020]	-	.777	.920	.829	.763	.909	.816	.942	.987	.959
	RNM [Zhu *et al.*, 2021]	-	.840	.919	.870	.872	.944	.899	.938	.981	.954
	CLEM† [Wu *et al.*, 2022]	-	.854	.935	.879	.885	.958	.904	.936	.977	.952
	RPR-RHGT [Cai *et al.*, 2022]	-	.693	-	.754	.886	-	.912	.889	-	.919
	ERMC† [Yang *et al.*, 2021]	-	.903	.946	.899	.942	.944	.925	.962	.982	.973
	EVA* [Liu *et al.*, 2021]	13.8M	.929	.986	.951	.964	.997	.976	.990	.999	.994
	MSNEA* [Chen *et al.*, 2022]	14.7M	.887	.961	.913	.938	.983	.955	.969	.997	.980
	MCLEA* [Lin *et al.*, 2022]	13.7M	.926	.983	.946	.961	.994	.973	.987	.999	.992
	MEAformer (Ours)	14.2M	**.948**	**.993**	**.965**	**.977**	**.999**	**.986**	**.991**	**1.00**	**.995**
	w/ MERP	14.2M	**.949**	**.993**	**.965**	**.978**	**.999**	**.986**	**.991**	**1.00**	**.995**
Unsup.	EVA* [Liu *et al.*, 2021]	13.8M	.883	.967	.913	.930	.985	.951	.968	.995	.978
	MSNEA* [Chen *et al.*, 2022]	14.7M	.858	.935	.886	.921	.973	.939	.953	.990	.967
	MCLEA* [Lin *et al.*, 2022]	13.7M	.879	.963	.909	.931	.983	.951	.959	.993	.972
	MEAformer (Ours)	14.2M	**.917**	**.980**	**.941**	**.958**	**.992**	**.972**	**.973**	**.998**	**.982**

Table 1: **Non-iterative** results without (w/o) and with (w/) surface forms (SF) on three **bilingual** datasets, where † denotes that the PLMs were applied for surface/attribute embedding generation. "Para." refers to the number of learnable parameters. "Unsup." refers to the unsupervised learning depended on entities' surface. The best results in baselines are marked with underline, and we highlight our results with **bold** when we achieve new SOTA. The symbol $*$ denotes our reproduced results on the same experiment setting.

scope of $\mathcal{N}_i^{ng}$ within the mini-batch. We define the alignment probability distribution as:

$$p_m(e_i^1, e_i^2) = \frac{\gamma_m(e_i^1, e_i^2)}{\gamma_m(e_i^1, e_i^2) + \sum_{e_j \in \mathcal{N}_i^{ng}} \gamma_m(e_i^1, e_j)}, \quad (14)$$

where $\gamma_m(e_i, e_j) = exp(h_i^{m\top} h_j^m / \tau)$ and τ is the temperature hyper-parameter. Considering the alignment direction for entity pairs reflected in (14), we define the bi-directional alignment objective for modality m as:

$$\mathcal{L}_m = -log(p_m(e_i^1, e_i^2) + p_m(e_i^2, e_i^1))/2\,. \quad (15)$$

We follow [Lin *et al.*, 2022] to introduce the intra-modal contrastive loss $\mathcal{L}_{ICL}$ which encourages the model to explicitly align the multi-modal future h^m. Moreover, we involve a late intra-modal contrastive loss $\mathcal{L}_{LICL}$ to realize the mutual information complementarity and the trade-offs among modalities via cross-modal knowledge transfer:

$$\mathcal{L}_{ICL} = \sum\nolimits_{m \in \mathcal{M}} \mathcal{L}_m,\ \mathcal{L}_{LICL} = \sum\nolimits_{m \in \mathcal{M}} \widehat{\mathcal{L}}_m, \quad (16)$$

where $\widehat{\mathcal{L}}_m$ is $\mathcal{L}_m$ variant with $\widehat{\gamma}_m(e_i, e_j) = exp(\hat{h}_i^{m\top} \hat{h}_j^m / \tau)$.

Finally, we train the network to minimize the overall loss:

$$\mathcal{L} = \mathcal{L}_\mu + \mathcal{L}_{ICL} + \mathcal{L}_{LICL}, \quad (17)$$

where $\mathcal{L}_\mu$ is based on the joint early fusion embedding h^μ.

Modal-aware Hard Entity Replay. To further improve the model's performance on those hard (i.e., very likely but not aligned) entity pairs with vague details, we develop a modal-aware entity replay (MERP) policy. Concretely, we require the model to not only passively sample in-batch negative but also proactively search for out-batch negative. To speed up the process, a hard negative matrix $\boldsymbol{M}_{neg} \in \mathbb{R}^{(|\mathcal{E}_1|+|\mathcal{E}_2|)\times 2}$ is adopted, where the nearest non-aligned target of each entity in the vector space is stored and updated after each training step. Then, those existing hard negative entities can be quickly retrieved to expand the original negative set through entity looking up in $\boldsymbol{M}_{neg}$ according to the mini-batch input entities. In order to mitigate the additional noise introduced by single modality divergence, MERP is only applied on the objective $\mathcal{L}_\mu$ for joint embedding.

4 Experiment

Our experiments cover model's performance on: *typical supervised scenario; unsupervised scenario; involving surface format's corpus; iterative training strategy; low resource scenario; convergence speed.* Please see appendix for details about different scenarios.

Note that all ablation / efficiency / case studies are conducted on typical supervised scenario unless otherwise specified. Moreover, we use the cosine similarity to measure the alignment probability, and multiple metrics including Hit@N (N=1, 10), MR (mean rank ↓), MRR (Mean Meciprocal Rank ↑) are adopted for evaluation.

4.1 Experiment Setup

Datasets. We consider two types of datasets. ***(i) Bilingual***: DBP15K [Sun *et al.*, 2017] contains three datasets built from the multilingual versions of DBpedia: DBP15K$_{ZH\text{-}EN}$, DBP15K$_{JA\text{-}EN}$ and DBP15K$_{FR\text{-}EN}$. Each of them contains

	Models	Para.	DBP15K$_{ZH-EN}$			DBP15K$_{JA-EN}$			DBP15K$_{FR-EN}$		
			H@1	H@10	MRR	H@1	H@10	MRR	H@1	H@10	MRR
w/o SF	BootEA [Sun *et al.*, 2018]	-	.629	.847	.703	.622	.854	.701	.653	.874	.731
	NAEA [Zhu *et al.*, 2019]	-	.650	.867	.720	.641	.873	.718	.673	.894	.752
	EVA* [Liu *et al.*, 2021]	13.3M	.746	.910	.807	.741	.918	.805	.767	.939	.831
	MSNEA* [Chen *et al.*, 2022]	14.1M	.643	.865	.719	.572	.832	.660	.584	.841	.671
	MCLEA* [Lin *et al.*, 2022]	13.2M	.811	.954	.865	.806	.953	.861	.811	.954	.865
	MEAformer (Ours)	13.7M	**.847**	**.970**	**.892**	**.842**	**.974**	**.892**	**.845**	**.976**	**.894**
w/ SF	EVA* [Liu *et al.*, 2021]	13.8M	.956	.993	.969	.979	.998	.987	.995	.999	.997
	MSNEA* [Chen *et al.*, 2022]	14.7M	.896	.969	.922	.942	.986	.958	.971	.998	.982
	MCLEA* [Lin *et al.*, 2022]	13.7M	.964	.996	.977	.986	.999	.992	.995	1.00	.997
	MEAformer (Ours)	14.2M	**.973**	**.998**	**.983**	**.991**	**1.00**	**.995**	**.996**	**1.00**	**.998**
Unsup.	EASY† [Ge *et al.*, 2021]	-	.898	.979	.930	.943	.990	.960	.980	.998	.990
	EVA* [Liu *et al.*, 2021]	13.8M	.937	.991	.957	.974	.998	.983	.992	1.00	.996
	MSNEA* [Chen *et al.*, 2022]	14.7M	.870	.946	.897	.933	.980	.950	.961	.992	.973
	MCLEA* [Lin *et al.*, 2022]	13.7M	.947	.995	.966	.977	.999	.986	.990	1.00	.994
	MEAformer (Ours)	14.2M	**.962**	**.998**	**.976**	**.987**	**.999**	**.992**	**.993**	**1.00**	**.996**

Table 2: Comparative results of our **iterative** models on three **bilingual** datasets.

	Models	FB15K-DB15K			FB15K-YAGO15K		
		H@1	H@10	MRR	H@1	H@10	MRR
20%	MMEA	.265	.541	.357	.234	.480	.317
	EVA∗	.199	.448	.283	.153	.361	.224
	MSNEA∗	.114	.296	.175	.103	.249	.153
	MCLEA∗	.295	.582	.393	.254	.484	.332
	MEAformer	**.417**	**.715**	**.518**	**.327**	**.595**	**.417**
	w/ MERP	**.434**	**.728**	**.534**	**.325**	**.598**	**.416**
50%	MMEA	.417	.703	.512	.403	.645	.486
	EVA∗	.334	.589	.422	.311	.534	.388
	MSNEA∗	.288	.590	.388	.320	.589	.413
	MCLEA∗	.555	.784	.637	.501	.705	.574
	MEAformer	**.619**	**.843**	**.698**	**.560**	**.778**	**.639**
	w/ MERP	**.625**	**.847**	**.704**	**.560**	**.780**	**.640**
80%	MMEA	.590	.869	.685	.598	.839	.682
	EVA∗	.484	.696	.563	.491	.692	.565
	MSNEA∗	.518	.779	.613	.531	.778	.620
	MCLEA∗	.735	.890	.790	.667	.824	.722
	MEAformer	**.765**	**.916**	**.820**	**.703**	**.873**	**.766**
	w/ MERP	**.773**	**.918**	**.825**	**.705**	**.874**	**.768**

Table 3: **Non-iterative** results on two **monolingual** datasets compared with other MMEA methods where *X*% represents the percentage of reference entity alignments used for training.

about 400K triples and 15K reference EA pairs with 30% as seed alignments for training. We adopt its multi-model variant [Liu *et al.*, 2021] with entity-matched images. ***(ii) Monolingual***: We select FB15K-DB15K (FBDB15K) and FB15K-YAGO15K (FBYG15K) in MMKG [Liu *et al.*, 2019] with three data splits which have 20%, 50%, and 80% of reference EA pairs as see alignments for training, respectively. Note that for the entity without image attached, a random vector is generated as its visual feature, following [Liu *et al.*, 2021]. Please see appendix for more dataset details.

Basic Baselines. 12 prominent EA algorithms proposed in recent years are selected as basic baselines. For a clear comparison, we divide them into four categories according to whether they are iterable and whether they use the surface format information. Correspondingly, we compare with them under the same setting.

Strong Baselines. We further collect five MMEA methods as the strong baselines, including CLEM [Wu *et al.*, 2022], MMEA [Chen *et al.*, 2020a], EVA [Liu *et al.*, 2021], MSNEA [Chen *et al.*, 2022], and MCLEA [Lin *et al.*, 2022]. Particularly, we reproduce EVA, MSNEA, and MCLEA with their original model pipelines unchanged.

	Models	FB15K-DB15K			FB15K-YAGO15K		
		H@1	H@10	MRR	H@1	H@10	MRR
20%	EVA∗	.231	.488	.318	.188	.403	.260
	MSNEA∗	.149	.392	.232	.138	.346	.21
	MCLEA∗	.395	.656	.487	.322	.546	.400
	MEAformer	**.578**	**.812**	**.661**	**.444**	**.692**	**.529**
50%	EVA∗	.364	.606	.449	.325	.560	.404
	MSNEA∗	.358	.656	.459	.376	.646	.472
	MCLEA∗	.620	.832	.696	.563	.751	.631
	MEAformer	**.690**	**.871**	**.755**	**.612**	**.808**	**.682**
80%	EVA∗	.491	.711	.573	.493	.695	.572
	MSNEA∗	.565	.810	.651	.593	.806	.668
	MCLEA∗	.741	.900	.802	.681	.837	.737
	MEAformer	**.784**	**.921**	**.834**	**.724**	**.880**	**.783**

Table 4: **Iterative** results on two **monolingual** datasets.

Implementation Details. Since those above works have various research focus and different experiment datasets, we reproduce them with the following settings to be consistent with our model for fairness[1]: ***(i)*** The hidden layer dimensions d for all networks are unified into 300. The total epochs are set to 500 with optional iterative training strategy applied on another 500 epochs, following [Lin *et al.*, 2022]. Training strategies including cosine warm-up schedule (15% steps for LR warm up), early stopping, and gradient accumulation are adopted. The AdamW optimizer ($\beta_1 = 0.9$, $\beta_2 = 0.999$) is adopted, and the batch size is fixed to 3500. ***(ii)*** To demonstrate model's stability, the vision encoders Enc_v are set to ResNet-152 [He *et al.*, 2016] on DBP15K following EVA/MCLEA where the vision feature dimension d_v is 2048, and set to VGG-16 [Simonyan and Zisserman, 2015] on FBDB15K/FBYG15K following MMEA [Chen *et al.*, 2020a] with $d_v = 4096$. ***(iii)*** Following [Yang *et al.*, 2019], the Bag-of-Words are selected for relations (x^r) and attributes (x^a) encoding where each entity has a fixed-length (e.g., $d_r = 1000$) vector for modal-

[1]The baselines reproduced with our settings partly have higher performance than their original.

ity feature representation. We follow [Lin *et al.*, 2022; Mao *et al.*, 2021] to use the pre-trained 300-d GloVe vectors together with the character bigrams for surface representation after applying entity name machine translations. ***(iv)*** An alignment editing method is employed to reduce the error accumulation [Sun *et al.*, 2018].

Specifically, for MEAformer, the FFN layer is removed from DCMW to simplify the model structure where the intermediate dimension d_{in} is set to 400. τ is set to 0.1, and the head number N_h in MHCA is set to 1. For MSNEA, we eliminate the attribute values used in MSNEA for input consistency, and extend MSNEA with iterative training ability.

We claim that the surface information will only be involved in bilingual datasets (DBP15K) following [Lin *et al.*, 2022], and we abandon those extra entity descriptions referred in minority EA works [Tang *et al.*, 2020]. All experiments are conducted on RTX 3090Ti GPUs.

4.2 Overall Results

The results of the bilingual datasets are shown in Table 1 (non-iterative) and Table 2 (iterative), and the results of the monolingual datasets are shown in Table 3 (non-iterative) and Table 4 (iterative). It is clear that our model has better performance than baselines across all the datasets under all the metrics. Particularly, MEAformer surpasses those methods on typical **supervised** scenario by a large margin on Hit@1 of DBP15K ($5 \sim 6\%$) and FBDB15K/FBYG15K ($3 \sim 11\%$), and consistently gains improvements on other settings over the SOTA methods with the number of learnable parameters (about 14M) being close to them.

It is reasonable that all models raise them performances when including the **surface** modality, since the textual messages are inherently a strong supervisory signal in alignment fields [Xu *et al.*, 2019]. Nevertheless, our model still exceeds the baselines with high performance, and increases the current SOTA Hit@1 scores from .929/.964/.990 to .948/.977/.991 on $ZH\text{-}EN$/$JA\text{-}EN$/$FR\text{-}EN$ of DBP15K, respectively. As an import application scene in real world, **unsupervised** MMEA, which is achieved by generating pseudo labeled seed alignments based on the similarity of the features extracted by the pre-trained model, could effectively get rid of the cost from manual labeling and annotation. Concretely, we follow [Lin *et al.*, 2022] to take entities' surface or visual features as the unsupervised references. Part of the results are illustrated in Table 1 and 2 with "Unsup." as the indication, where our MEAformer achieves the SOTA results with surface forms as a basis. Please see appendix for more detailed results based on visual forms.

Moreover, we note that the **MERP** policy could further increase model's performances among all datasets but it is not involved in our standard MEAformer, since we hope to disengage it from the model and make it a generic technique for EA methods. Note that we abandon MERP when training model with iterative or unsupervised strategy since the generated pseudo seed alignments is not absolutely correct which may mislead the model and cause the error cascade issue.

Efficiency Analysis. To get further insights into our model, we report the efficiency behaviors of four MMEA algorithms on two datasets with identical 3000 epochs and early stopping strategy. As shown in Figure 3, MEAformer consistently outperforms others throughout the training progress (left), and it is also superior in the trade-off between convergence time and performance (right). We own MSNEA's poor behavior to the fact that the translation-based models are constrained by their geometric models which limits their abilities to capture complex structural relationships among entities for EA [Yang *et al.*, 2021]. Please see appendix for details.

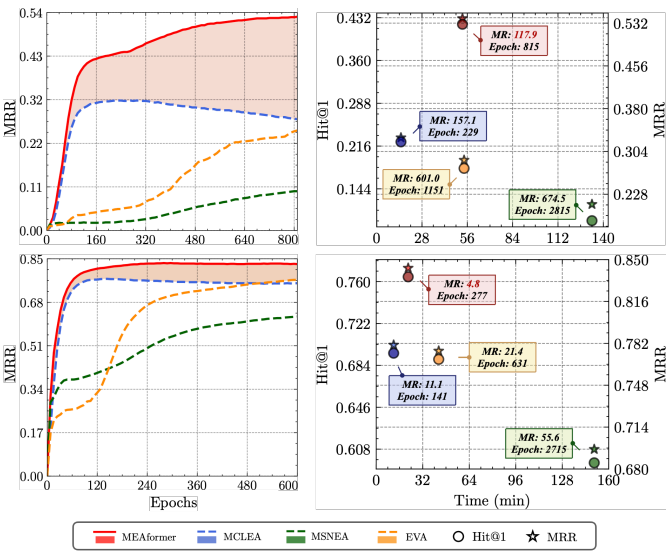

Figure 3: **Efficiency Analysis.** Performance $vs.$ training epoches (left), and performance $vs.$ training time (right), on 20% seeds FBDB15K (up) and DBP15K$_{ZH-EN}$ (down).

4.3 Ablation Studies

Low Resource. To discuss the model's stability on fewer seed alignments, we evaluate MEAformer on two datasets with seed alignment ratio (R_{sa}) ranging from 0.01 to 0.20 in FBDB15K and from 0.01 to 0.30 in DBP15K$_{FR-EN}$. Figure 4 presents a clear gap that persists throughout the ratio increasing, which grows bigger when the R_{sa} is over about 0.1. It is worth noting that MEAformer can even achieve .392 on Hit@1 in DBP15K$_{FR\text{-}EN}$ with only 1% seed alignments, compared with .344 for MCLEA, showing our potential for few-shot EA, which is among our future works.

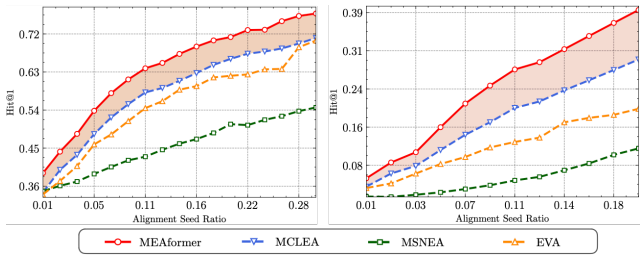

Figure 4: **Low Resource.** Models' performance with fewer seed alignments on DPB15K$_{FR\text{-}EN}$ (left) and FBDB15K (right).

Component Analysis. We evaluate various stripped-down versions of MEAformer in Figure 5 to show the Hit@1/MRR gains brought by different components. Concretely, we find

that removing the content from either modality always leads to a noticeable performance degradation, especially the vision. We hypothesize that the attribute and relation modalities may have certain information complementarity and a coupling association exists between them to some extent, e.g., as the first case in Figure 1 presents, *clubs* and *national_team* both appear in $\mathcal{A}$ and $\mathcal{R}$ set of entity *Mario Gomez*, which is partially redundant.

Besides, the training objectives, including $\mathcal{L}_{ICL}$, $\mathcal{L}_{LICL}$ and $\mathcal{L}_{\mu}$, all clearly boost the performance, which demonstrates the effectiveness of our training target. Note that an extra objective $\mathcal{L}_{\xi}$, which is $\mathcal{L}_{\mu}$'s variant with late fusion embedding as the entity feature in (13), can slightly enhance our model. We guess that the reason for $\mathcal{L}_{\xi}$'s insignificant improvement comes from the mutually modality iteration in MHCA, which leads to a decline in the contribution of late fusion to the overall training. This is supported by the performance degradation when removing $\mathcal{L}_{ICL}$ compared with $\mathcal{L}_{LICL}$ (i.e., the former's impact is bigger). So, we simply abandon $\mathcal{L}_{\xi}$ for higher model efficiency. Lastly, we claim that FFN is an essential part in the bilingual datasets from DBP15K while we do not observe the performance improvement on the monolingual datasets.

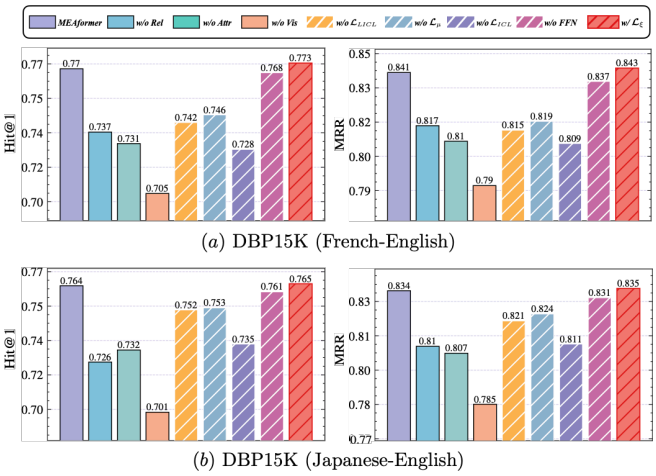

(*a*) DBP15K (French-English)

(*b*) DBP15K (Japanese-English)

Figure 5: **Component Analysis** for MEAformer on DBP15K$_{FR\text{-}EN}$ (up) and DBP15K$_{JA\text{-}EN}$ (down).

4.4 Details Analysis

Error Analysis. To discuss MEAformer's robustness, we compare it with EVA via recording the prediction distribution of four times evaluations (with variant random seeds) in DBP15K. Concretely, we defines an entity as an unanimously correct entity (e_{uc}) when it is aligned successfully across all evaluations. We observe that the Hit@1 e_{uc} (.762/.751/.761) for MEAformer are close to the original results .771/.764/.770 in three datasets. While for EVA, they drop from .680/.673/.683 to .490/.531/.575, which are less stable than ours. Moreover, in Figure 6 we visualize the two models' prediction intersection to compare model's mutual error correction ability. We see that MEAformer correctly predicts 57.56%/46.89%/42.56% of the entities that EVA wrongly predicts, while EVA only correctly predicts 9.1%/12.9%/10.1% of the entities that MEAformer wrongly predicts.

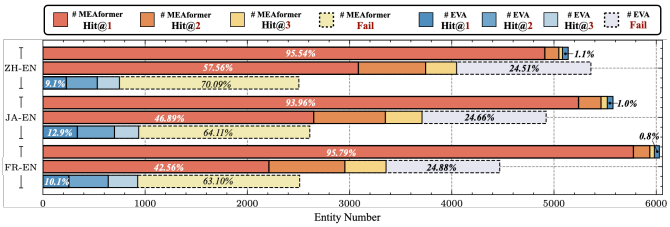

Figure 6: **Error Analysis** in DBP15K where "# Hit@N" refers to the number of entities e_{uc} ranked in model's top n list, and "# Fail" refers to the the number of e_{uc} that model failed in.

Modality Distribution. In Figure 7 we analyze the distribution for modality weight. EVA's weight distribution suggests that the graph modality is extreme important while the weights for other modalities are relatively average and low. In contrast, the overall averaged distribution of our generated meta modal weights is flatter as shown in Figure 7(a). Meanwhile, we record the number of entities which reach the highest proportion in each modality (or combination of two modalities), in Figure 7(b). We find that although the averaged weights are smooth, a specific distribution of modal importance for different instances still exists which is similar to EVA's modality weight. This partly support our motivations in modality adaptation where the global (KG-level) and local (instance-level) weight optimum are realized simultaneously.

Several representative examples are shown in Figure 1 with their modality information attached in. Besides, more entity examples that achieve the highest score in corresponding modalities are presented in the appendix where a further analysis is conducted.

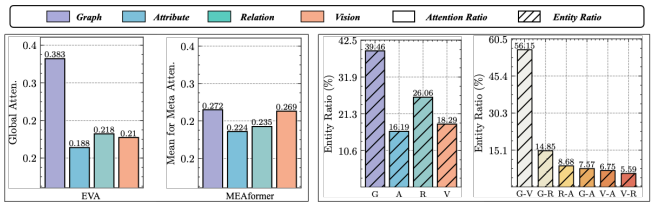

(*a*) Attention Weight on JA-EN.

(*b*) Entity distribution in each modality.

Figure 7: **Modality Distribution** for EVA and our MEAformer.

5 Conclusion

In this work, we have studied meta modality hybrid as an alternative strategy for multi-modal entity alignment with modified transformer architecture involved in. We have shown that our proposed MEAformer could not only outperforms in benchmarks across multiple aspects including typical supervised scenario; unsupervised scenario; involving surface format's corpus; iterative training strategy; low resource scenario; convergence speed, but also has good interpretability. Most importantly, our model is easy to follow and compatible with different modality formats, which could directly replace existing algorithm without major modifications.

References

[Bordes *et al.*, 2013] Antoine Bordes, Nicolas Usunier, Alberto García-Durán, Jason Weston, and Oksana Yakhnenko. Translating embeddings for modeling multi-relational data. In *NIPS*, pages 2787–2795, 2013.

[Cai *et al.*, 2022] Weishan Cai, Wenjun Ma, Jieyu Zhan, and Yuncheng Jiang. Entity alignment with reliable path reasoning and relation-aware heterogeneous graph transformer. In *IJCAI*, pages 1930–1937. ijcai.org, 2022.

[Cao *et al.*, 2019] Yixin Cao, Zhiyuan Liu, Chengjiang Li, Juanzi Li, and Tat-Seng Chua. Multi-channel graph neural network for entity alignment. In *ACL (1)*, pages 1452–1461. Association for Computational Linguistics, 2019.

[Chen *et al.*, 2020a] Liyi Chen, Zhi Li, Yijun Wang, Tong Xu, Zhefeng Wang, and Enhong Chen. MMEA: entity alignment for multi-modal knowledge graph. In *KSEM (1)*, volume 12274 of *Lecture Notes in Computer Science*, pages 134–147. Springer, 2020.

[Chen *et al.*, 2020b] Ting Chen, Simon Kornblith, Mohammad Norouzi, and Geoffrey E. Hinton. A simple framework for contrastive learning of visual representations. In *ICML*, volume 119 of *Proceedings of Machine Learning Research*, pages 1597–1607. PMLR, 2020.

[Chen *et al.*, 2021] Zhuo Chen, Jiaoyan Chen, Yuxia Geng, Jeff Z. Pan, Zonggang Yuan, and Huajun Chen. Zero-shot visual question answering using knowledge graph. In *ISWC*, volume 12922 of *Lecture Notes in Computer Science*, pages 146–162. Springer, 2021.

[Chen *et al.*, 2022] Liyi Chen, Zhi Li, Tong Xu, Han Wu, Zhefeng Wang, Nicholas Jing Yuan, and Enhong Chen. Multi-modal siamese network for entity alignment. In *KDD*, pages 118–126. ACM, 2022.

[Devlin *et al.*, 2019] Jacob Devlin, Ming-Wei Chang, Kenton Lee, and Kristina Toutanova. BERT: pre-training of deep bidirectional transformers for language understanding. In *NAACL-HLT (1)*, pages 4171–4186. Association for Computational Linguistics, 2019.

[Gao *et al.*, 2022a] Chen Gao, Xiang Wang, Xiangnan He, and Yong Li. Graph neural networks for recommender system. In *WSDM*, pages 1623–1625. ACM, 2022.

[Gao *et al.*, 2022b] Yunjun Gao, Xiaoze Liu, Junyang Wu, Tianyi Li, Pengfei Wang, and Lu Chen. Clusterea: Scalable entity alignment with stochastic training and normalized mini-batch similarities. In *KDD*, pages 421–431. ACM, 2022.

[Ge *et al.*, 2021] Congcong Ge, Xiaoze Liu, Lu Chen, Baihua Zheng, and Yunjun Gao. Make it easy: An effective end-to-end entity alignment framework. In *SIGIR*, pages 777–786. ACM, 2021.

[Geng *et al.*, 2021] Yuxia Geng, Jiaoyan Chen, Zhuo Chen, Jeff Z. Pan, Zhiquan Ye, Zonggang Yuan, Yantao Jia, and Huajun Chen. Ontozsl: Ontology-enhanced zero-shot learning. In *WWW*, pages 3325–3336. ACM / IW3C2, 2021.

[He *et al.*, 2016] Kaiming He, Xiangyu Zhang, Shaoqing Ren, and Jian Sun. Deep residual learning for image recognition. In *CVPR*, pages 770–778. IEEE Computer Society, 2016.

[Hospedales *et al.*, 2022] Timothy M. Hospedales, Antreas Antoniou, Paul Micaelli, and Amos J. Storkey. Meta-learning in neural networks: A survey. *IEEE Trans. Pattern Anal. Mach. Intell.*, 44(9):5149–5169, 2022.

[Jiménez-Ruiz and Grau, 2011] Ernesto Jiménez-Ruiz and Bernardo Cuenca Grau. Logmap: Logic-based and scalable ontology matching. In *ISWC (1)*, volume 7031 of *Lecture Notes in Computer Science*, pages 273–288. Springer, 2011.

[Kipf and Welling, 2017] Thomas N. Kipf and Max Welling. Semi-supervised classification with graph convolutional networks. In *ICLR (Poster)*. OpenReview.net, 2017.

[Li *et al.*, 2019] Chengjiang Li, Yixin Cao, Lei Hou, Jiaxin Shi, Juanzi Li, and Tat-Seng Chua. Semi-supervised entity alignment via joint knowledge embedding model and cross-graph model. In *EMNLP/IJCNLP (1)*, pages 2723–2732. Association for Computational Linguistics, 2019.

[Lin *et al.*, 2022] Zhenxi Lin, Ziheng Zhang, Meng Wang, Yinghui Shi, Xian Wu, and Yefeng Zheng. Multi-modal contrastive representation learning for entity alignment. In *COLING*, pages 2572–2584. International Committee on Computational Linguistics, 2022.

[Liu *et al.*, 2019] Ye Liu, Hui Li, Alberto García-Durán, Mathias Niepert, Daniel Oñoro-Rubio, and David S. Rosenblum. MMKG: multi-modal knowledge graphs. In *ESWC*, volume 11503 of *Lecture Notes in Computer Science*, pages 459–474. Springer, 2019.

[Liu *et al.*, 2020] Zhiyuan Liu, Yixin Cao, Liangming Pan, Juanzi Li, and Tat-Seng Chua. Exploring and evaluating attributes, values, and structures for entity alignment. In *EMNLP (1)*, pages 6355–6364. Association for Computational Linguistics, 2020.

[Liu *et al.*, 2021] Fangyu Liu, Muhao Chen, Dan Roth, and Nigel Collier. Visual pivoting for (unsupervised) entity alignment. In *AAAI*, pages 4257–4266. AAAI Press, 2021.

[Mao *et al.*, 2021] Xin Mao, Wenting Wang, Yuanbin Wu, and Man Lan. From alignment to assignment: Frustratingly simple unsupervised entity alignment. In *EMNLP (1)*, pages 2843–2853. Association for Computational Linguistics, 2021.

[Simonyan and Zisserman, 2015] Karen Simonyan and Andrew Zisserman. Very deep convolutional networks for large-scale image recognition. In *ICLR*, 2015.

[Suchanek *et al.*, 2011] Fabian M. Suchanek, Serge Abiteboul, and Pierre Senellart. PARIS: probabilistic alignment of relations, instances, and schema. *Proc. VLDB Endow.*, 5(3):157–168, 2011.

[Sun *et al.*, 2017] Zequn Sun, Wei Hu, and Chengkai Li. Cross-lingual entity alignment via joint attribute-preserving embedding. In *ISWC (1)*, volume 10587 of *Lec-*

ture Notes in Computer Science, pages 628–644. Springer, 2017.

[Sun *et al.*, 2018] Zequn Sun, Wei Hu, Qingheng Zhang, and Yuzhong Qu. Bootstrapping entity alignment with knowledge graph embedding. In *IJCAI*, pages 4396–4402. ijcai.org, 2018.

[Sun *et al.*, 2019] Zequn Sun, Jiacheng Huang, Wei Hu, Muhao Chen, Lingbing Guo, and Yuzhong Qu. Transedge: Translating relation-contextualized embeddings for knowledge graphs. In *ISWC (1)*, volume 11778 of *Lecture Notes in Computer Science*, pages 612–629. Springer, 2019.

[Sun *et al.*, 2020] Zequn Sun, Chengming Wang, Wei Hu, Muhao Chen, Jian Dai, Wei Zhang, and Yuzhong Qu. Knowledge graph alignment network with gated multi-hop neighborhood aggregation. In *AAAI*, pages 222–229. AAAI Press, 2020.

[Tang *et al.*, 2020] Xiaobin Tang, Jing Zhang, Bo Chen, Yang Yang, Hong Chen, and Cuiping Li. BERT-INT: A bert-based interaction model for knowledge graph alignment. In *IJCAI*, pages 3174–3180. ijcai.org, 2020.

[Trisedya *et al.*, 2019] Bayu Distiawan Trisedya, Jianzhong Qi, and Rui Zhang. Entity alignment between knowledge graphs using attribute embeddings. In *AAAI*, pages 297–304. AAAI Press, 2019.

[Vaswani *et al.*, 2017] Ashish Vaswani, Noam Shazeer, Niki Parmar, Jakob Uszkoreit, Llion Jones, Aidan N. Gomez, Lukasz Kaiser, and Illia Polosukhin. Attention is all you need. In *NIPS*, pages 5998–6008, 2017.

[Velickovic *et al.*, 2018] Petar Velickovic, Guillem Cucurull, Arantxa Casanova, Adriana Romero, Pietro Liò, and Yoshua Bengio. Graph attention networks. In *ICLR (Poster)*. OpenReview.net, 2018.

[Wu *et al.*, 2019] Yuting Wu, Xiao Liu, Yansong Feng, Zheng Wang, Rui Yan, and Dongyan Zhao. Relation-aware entity alignment for heterogeneous knowledge graphs. In *IJCAI*, pages 5278–5284. ijcai.org, 2019.

[Wu *et al.*, 2020] Yuting Wu, Xiao Liu, Yansong Feng, Zheng Wang, and Dongyan Zhao. Neighborhood matching network for entity alignment. In *ACL*, pages 6477–6487. Association for Computational Linguistics, 2020.

[Wu *et al.*, 2022] Tianxing Wu, Chaoyu Gao, Lin Li, and Yuxiang Wang. Leveraging multi-modal information for cross-lingual entity matching across knowledge graphs. *Applied Sciences*, 12(19):10107, 2022.

[Xiang *et al.*, 2021] Yuejia Xiang, Ziheng Zhang, Jiaoyan Chen, Xi Chen, Zhenxi Lin, and Yefeng Zheng. Ontoea: Ontology-guided entity alignment via joint knowledge graph embedding. In Chengqing Zong, Fei Xia, Wenjie Li, and Roberto Navigli, editors, *Findings of the Association for Computational Linguistics: ACL/IJCNLP 2021, Online Event, August 1-6, 2021*, volume ACL/IJCNLP 2021 of *Findings of ACL*, pages 1117–1128. Association for Computational Linguistics, 2021.

[Xin *et al.*, 2022] Kexuan Xin, Zequn Sun, Wen Hua, Wei Hu, and Xiaofang Zhou. Informed multi-context entity alignment. In *WSDM*, pages 1197–1205. ACM, 2022.

[Xu *et al.*, 2019] Kun Xu, Liwei Wang, Mo Yu, Yansong Feng, Yan Song, Zhiguo Wang, and Dong Yu. Cross-lingual knowledge graph alignment via graph matching neural network. In *ACL (1)*, pages 3156–3161. Association for Computational Linguistics, 2019.

[Yang *et al.*, 2015] Bishan Yang, Wen-tau Yih, Xiaodong He, Jianfeng Gao, and Li Deng. Embedding entities and relations for learning and inference in knowledge bases. In *ICLR (Poster)*, 2015.

[Yang *et al.*, 2019] Hsiu-Wei Yang, Yanyan Zou, Peng Shi, Wei Lu, Jimmy Lin, and Xu Sun. Aligning cross-lingual entities with multi-aspect information. In *EMNLP/IJCNLP (1)*, pages 4430–4440. Association for Computational Linguistics, 2019.

[Yang *et al.*, 2021] Jinzhu Yang, Ding Wang, Wei Zhou, Wanhui Qian, Xin Wang, Jizhong Han, and Songlin Hu. Entity and relation matching consensus for entity alignment. In *CIKM*, pages 2331–2341. ACM, 2021.

[Zeng *et al.*, 2020] Weixin Zeng, Xiang Zhao, Jiuyang Tang, and Xuemin Lin. Collective entity alignment via adaptive features. In *ICDE*, pages 1870–1873. IEEE, 2020.

[Zhang *et al.*, 2019] Qingheng Zhang, Zequn Sun, Wei Hu, Muhao Chen, Lingbing Guo, and Yuzhong Qu. Multi-view knowledge graph embedding for entity alignment. In *IJCAI*, pages 5429–5435. ijcai.org, 2019.

[Zhang *et al.*, 2022] Rui Zhang, Bayu Distiawan Trisedya, Miao Li, Yong Jiang, and Jianzhong Qi. A benchmark and comprehensive survey on knowledge graph entity alignment via representation learning. *VLDB J.*, 31(5):1143–1168, 2022.

[Zhong *et al.*, 2022] Ziyue Zhong, Meihui Zhang, Ju Fan, and Chenxiao Dou. Semantics driven embedding learning for effective entity alignment. In *ICDE*, pages 2127–2140. IEEE, 2022.

[Zhu *et al.*, 2017] Hao Zhu, Ruobing Xie, Zhiyuan Liu, and Maosong Sun. Iterative entity alignment via joint knowledge embeddings. In *IJCAI*, pages 4258–4264. ijcai.org, 2017.

[Zhu *et al.*, 2019] Qiannan Zhu, Xiaofei Zhou, Jia Wu, Jianlong Tan, and Li Guo. Neighborhood-aware attentional representation for multilingual knowledge graphs. In *IJCAI*, pages 1943–1949. ijcai.org, 2019.

[Zhu *et al.*, 2021] Yao Zhu, Hongzhi Liu, Zhonghai Wu, and Yingpeng Du. Relation-aware neighborhood matching model for entity alignment. In *AAAI*, pages 4749–4756. AAAI Press, 2021.

A Appendix

A.1 Dataset Statistics

Our detailed dataset statistics are presented in Table 5, which are consistent with [Lin *et al.*, 2022]. Note that those remained non-training seed alignments are set for testing.

A.2 Supplementary for Baselines

Attribute Value. Those attribute triples <*entity*, *attribute*, *value*> in KGs have been researched in many previous works [Trisedya *et al.*, 2019; Liu *et al.*, 2020; Tang *et al.*, 2020; Chen *et al.*, 2022; Zhong *et al.*, 2022]. Nevertheless, in order to focus on our key subject, we do not utilize the contents of *value* parts in our work which are mainly string formats like specific date, land area or coordinate position. Moreover, our MEAformer still exceeds those methods on performance with vision modality involved in.

PLM-based Co-training. As shown in Table 6, Our model also outperforms those PLM-based co-training EA methods which fine-tune the PLMs (e.g., BERT [Devlin *et al.*, 2019]) during or before model training. Note that their learnable parameters ($>$ 110M) are much huge than MEAformer (14M). The results for baselines are excerpted from [Zhong *et al.*, 2022] where the BERT-INT [Tang *et al.*, 2020] is reproduced with entity descriptions removed. Note that the attribute values is involved in those two algorithms but absent in ours.

Baseline Analysis. We own the lower performance of translation-based methods (e.g., MSNEA) to the reason that most of them are constrained by their semantics assumption, failing to capture complex structural information among entities for alignment. [Wu *et al.*, 2019; Yang *et al.*, 2021] hold that structural information plays an important role in the EA task. By performing graph convolution over an entity's neighbors, GCN is able to capture more structural characteristics of knowledge graphs, while the translation assumption in translation-based models focuses more on the relationship among heads, tails and relations.

Moreover, with the increase of modalities (e.g., surface) and the enrichment of modal semantic information (e.g., embedding from PLMs), the EA performance will always be improved. This supports that our MEAformer has great potential since it achieves state-of-the-art results without relying on pre-trained language models and extra surface from attributes/values. Most importantly, this further demonstrates that the MMKG can promote the development of EA in the future from another multi-modal aspect.

A.3 Training Details

Iterative Training. We follow [Lin *et al.*, 2022] to adopt a probation technique for iterative Training. Concretely, each pair of cross-graph entities that are mutual nearest neighbours in vector space is proposed and added into a candidate list for every K_e ($= 5$) epochs. A proposed entity pair will be added into the training set if it remains mutual nearest neighbours throughout K_s ($= 10$) consecutive rounds.

Efficiency Analysis Specifically, we set the total epochs for each model into 3000 with early stopping rule adopted to get the *best achievable* performances, because more epochs will make the learning rate change smoother with warm-up schedule. We observe that this setting help further increase our performances on FBDB15K (20% seed alignments) from $.417/.518$ to $.431/.530$ (Hit@1 / MRR), and increase our performances on DBP15K$_{ZH\text{-}EN}$ from $.771/.835$ to $.773/.837$.

A.4 Unsupervised Training with Vision Modality

Unsupervised MMEA is first proposed in [Liu *et al.*, 2021], which leverages the visual similarity of entities to create an pseudo seed dictionary ($\mathcal{S}_{dic}$) to avoid the reliance on gold labels. Not that $\mathcal{S}_{dic}$ is a set of seed alignments which is initialized with an empty collection and a predefined maximum size (N_{dic}) firstly. Then the algorithm will fill the dictionary $\mathcal{S}_{dic}$ to length N_{dic} ($|\mathcal{S}_{dic}| = N_{dic}$) based on the sorted similarity of entity's pre-extract modality features

As elaborated in Section 4.2, we take entities' surface or visual features as the references and present the **surface-based results** on Table 1 and 2. In this section we complete the vision-based results in Table 7, demonstrating that MEAformer could stably achieve the SOTA unsupervised performance with different auxiliary modalities.

A.5 Case Supplementary

The modality analysis specified on Section 4.4 proves that entities indeed exist diverse distributions of modality weight across the MMKGs. In order to explore the influence of entity's modality traits on weight preference, we further analyze those entities with extreme unbalanced weights. Several examples are shown in Figure 1 with their modality information attached in. More cases from three bilingual datasets are recorded in Table 8, where those *(sports) athletes* or *(film) stars* generally have a stronger overall dependence on vision and graph (structure) modalities. We hypothesize that it's because they appearance characteristics and visual background are usually more recognizable. Besides, those *military* or *political* related entities are often highly dependent on relation modality as the case shown in 2/4 of Figure 1. We own this to the fact that the relationships among these types of entities are often more complex and diverse. Moreover, the noise involved in some modalities sometimes may interfere with the model judgment like the *arena lviv* in case 3 where the lawn visual pattern may offer only limited help, and case 2 where multiple dissimilar image of air force emblem refer to the same entity. Also, we observe that those entities with high confidence in graph (structure) modality is KG-specific. Specifically, we summarize the correspondence as follow:

- Football players (e.g., *David_Vill*) $-$ DBP15K$_{ZH\text{-}EN}$.
- Constellations (e.g., *Ursa_Major*) $-$ DBP15K$_{JA\text{-}EN}$.
- Switzerland's areas (e.g., *Crissier*) $-$ DBP15K$_{FR\text{-}EN}$.

We find that they tend to meet the following characteristics compared to other entities: ***(i)*** Larger node degree (i.e., the number of edges linked to the entity). ***(ii)*** Limited relation types. ***(iii)*** Associated entities are mostly of the same type or the same level on ontology [Geng *et al.*, 2021] (i.e., the graph is similar to a social network).

Dataset	KG	# Ent.	# Rel.	# Attr.	# Rel. Triples	# Attr. Triples	# Image	# Ref. EA
DBP15K$_{ZH-EN}$	ZH (Chinese)	19,388	1,701	8,111	70,414	248,035	15,912	15,000
	EN (English)	19,572	1,323	7,173	95,142	343,218	14,125	
DBP15K$_{JA-EN}$	JA (Japanese)	19,814	1,299	5,882	77,214	248,991	12,739	15,000
	EN (English)	19,780	1,153	6,066	93,484	320,616	13,741	
DBP15K$_{FR-EN}$	FR (French)	19,661	903	4,547	105,998	273,825	14,174	15,000
	EN (English)	19,993	1,208	6,422	115,722	351,094	13,858	
FBDB15K	FB15K	14,951	1,345	116	592,213	29,395	13,444	12,846
	DB15K	12,842	279	225	89,197	48,080	12,837	
FBYG15K	FB15K	14,951	1,345	116	592,213	29,395	13,444	11,199
	YAGO15K	15,404	32	7	122,886	23,532	11,194	

Table 5: Statistics for datasets, where "Ref. EA" refers to the reference entity alignments. Note that not all entities have the associated images or the equivalent counterparts in the other KG.

	Models	Para.	DBP15K$_{ZH-EN}$			DBP15K$_{JA-EN}$			DBP15K$_{FR-EN}$		
			H@1	H@10	MRR	H@1	H@10	MRR	H@1	H@10	MRR
w/ SF	BERT-INT [Tang *et al.*, 2020]	>110M	.814	.837	.820	.806	.835	.820	.987	.992	.990
	SDEA [Zhong *et al.*, 2022]	>110M	.870	.966	.910	.848	.952	.890	.969	.995	.980
	MEAformer (Ours)	**14.2M**	**.948**	**.993**	**.965**	**.977**	**.999**	**.986**	**.991**	**1.00**	**.995**

Table 6: Results of our **non-iterative** models on three **bilingual** datasets compared with those **PLM-based** co-training or fine-tuning methods. Note that entity descriptions are not available in all datasets for fairness.

	Models	Para.	DBP15K$_{ZH-EN}$			DBP15K$_{JA-EN}$			DBP15K$_{FR-EN}$		
			H@1	H@10	MRR	H@1	H@10	MRR	H@1	H@10	MRR
w/o Iter.	EVA* [Liu *et al.*, 2021]	13.8M	.891	.961	.917	.941	.986	.958	.970	996	.982
	MSNEA* [Chen *et al.*, 2022]	14.7M	.859	.936	.887	.921	.970	.939	.954	.989	.968
	MCLEA* [Lin *et al.*, 2022]	13.7M	.860	.950	.893	.914	.975	.938	.953	.990	.967
	MEAformer (Ours)	14.2M	**.909**	**.974**	**.933**	**.950**	**.990**	**.965**	**.972**	**.997**	**.983**
w/ Iter.	EVA* [Liu *et al.*, 2021]	13.8M	.948	.992	.964	.977	.997	.985	.990	1.00	.995
	MSNEA* [Chen *et al.*, 2022]	14.7M	.871	.943	.898	.927	.976	.945	.959	.993	.979
	MCLEA* [Lin *et al.*, 2022]	13.7M	.942	.994	.963	.974	.999	.984	.986	1.00	.992
	MEAformer (Ours)	14.2M	**.964**	**.998**	**.975**	**.985**	**1.00**	**.991**	**.992**	**1.00**	**.996**

Table 7: Unsupervised results of our MEAformer on three bilingual datasets based on **vision modality** without (w/o) and with (w/) iterative version (Iter.) against strong baseline methods on three bilingual datasets, where "Para." refers to the number of learnable parameters. The best results in baselines are marked with underline, and we highlight our results with **bold** when we achieve new SOTA. The symbol $*$ denotes the reproduced results on the same experiment setting.

Modality	**Examples**
Vision	`Feng_Renliang, Rivaldo, Reinaldo_da_Cruz_Oliveira, Gilberto_Silva, Didier_Zokora, Costinha, Kate_Bush, Billie_Jean, Take_My_Breath_Away, Léon_Blum, Celine_Dion, Ophiuchus, Lacerta`
Attribute	`Kingdom_of_England, Roman Republic, Timurid_Empire, Brown_University, 2014_AFC_Cup, 2015–16_Football_League_Cup, Kuwait_City, Calabria, Hong_Kong, Amsterdam, Hamburg, Kiev`
Relation	`United_States, France, Michael_Jackson, The_Beatles, Sony_Mobile, Microsoft, Apple_Inc, Queen_Victoria, Akihito, European_People's_Party, English_language, Aramaic_alphabet`
Graph	`Vágner_Love, David_Villa, Jimmy_Bullard, Torsten_Frings, Hydra_(constellation), Ursa_Major, Montricher, Delphinus, Scorpius, Volans, Locarno, Crissier, Schmiedrued, Tramelan`

Table 8: Part of the representative examples whose meta weights of corresponding modalities rank relatively high.

A.6 Low Resource Supplementary

we evaluate MEAformer with seed alignment ratio (R_{sa}) *[0.01, 0.02, 0.03, 0.05, 0.07, 0.09, 0.11, 0.12, 0.14, 0.16, 0.18, 0.20]* in FBDB15K and *[0.01, 0.02, 0.03, 0.05, 0.07, 0.09, 0.11, 0.12, 0.14, 0.16, 0.18, 0.20, 0.22, 0.24, 0.26, 0.28, 0.30]* in DBP15K$_{FR-EN}$. The hit@1 results are shown in Figure 4, and we present the MRR/MR results in in Figure 8. These trends all demonstrate the superiority of our model.

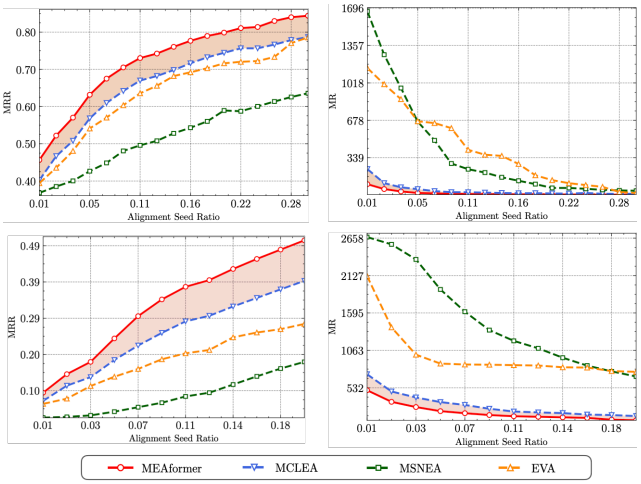

Figure 8: Models' MRR↑/MR↓ performance with fewer seed alignments on DPB15K$_{FR\text{-}EN}$ (up) and FBDB15K (down).

A.7 Baseline Reproducing

We reproduce EVA, MSNEA, and MCLEA based on their source code [2][3][4] with their original model pipelines unchanged.

[2] https://github.com/cambridgeltl/eva
[3] https://github.com/lzxlin/MCLEA
[4] https://github.com/liyichen-cly/MSNEA